Original Article

Evaluating the Theory Underpinning Nonlinear Raman Spectroscopy Methods: Stimulated Raman Scattering (SRS)and Coherent Anti-Stokes Raman Scattering (CARS)

Abullais Nehal Ahmed
Department of Physics, J.A.T. Arts, Science and Comm. College (for Women), Malegaon, Dist. Nashik, Maharashtra, India

Manuscript ID:
IJERSD-2025-010615

ISSN: 3067-2325

Volume 1

Issue 6

Pp 67-71

December 2025

Submitted: 10 Nov. 2025

Revised: 25 Nov. 2025

Accepted: 15 Dec 2025

Published: 31 Dec 2025

Correspondence Address:
Abullais Nehal Ahmed
Department of Physics, J.A.T. Arts, Science and Comm. College (for Women), Malegaon, Dist. Nashik, Maharashtra, India
Email: aabullais@gmail.com

Quick Response Code:

Web. https://rlgjaar.com

DOI: 10.5281/zenodo.18277118

DOI Link:
https://doi.org/10.5281/zenodo.18277118

Abstract:

The theoretical underpinnings of nonlinear Raman spectroscopy methods are examined in this work, with particular attention to coherent anti-Stokes Raman scattering (CARS) and stimulated Raman scattering (SRS). These cutting-edge methods improve molecular analysis's sensitivity and specificity by taking advantage of nonlinear optical phenomena. Line imaging, global or wide-field imaging, and sequential registration using laser scanning microscopes are some of the imaging techniques[13]. Despite obstacles like nonresonant background interference, CARS provides high-resolution imaging by using three laser beams to create a coherent anti-Stokes signal[8,12]. Recent developments have addressed these restrictions, such as deep learning techniques, which have improved spectral clarity. SRS, on the other hand, requires complex laser synchronization but provides background-free signals with greater chemical specificity by measuring changes in intensity brought on by vibrational excitations. Advancements in theory for both methods have broadened their uses in domains like materials science, real-time diagnostics, and live-cell imaging. To provide a comparative analysis that will direct future applications in scientific research, this investigation attempts to present the most recent research on these techniques and their theoretical foundations.

Keywords: *Stokes, anti-Stokes, coherent, stimulation, synchronization, imaging, interference, domain, etc.*

Introduction:

Nonlinear Raman spectroscopy encompasses techniques that leverage nonlinear optical effects to probe molecular vibrations beyond the linear regime of spontaneous Raman scattering[1,2]. Among these, Stimulated Raman Scattering (SRS) stands out as a coherent process that amplifies weak Raman signals through the interaction of pump and Stokes laser beams[4]. Discovered in 1962, SRS has evolved into a cornerstone for label-free chemical imaging, particularly in biological and materials applications[9].The theory underpinning SRS is rooted in quantum mechanical descriptions of light-matter interactions, where the frequency difference between the pump (ω_p) and Stokes (ω_S) beams matches a molecular vibrational mode ($\Omega = \omega_p - \omega_S$). This resonant enhancement leads to energy transfer, manifesting as gain in the Stokes beam and loss in the pump. Evaluating this theory involves examining its mathematical rigor, predictive accuracy, and practical limitations, as evidenced by recent theoretical estimations and experimental validations[10,13].Nonlinear Raman spectroscopy represents a significant advancement over traditional spontaneous Raman techniques by leveraging nonlinear optical interactions to achieve coherent, amplified signals. Coherent Anti-Stokes Raman Scattering (CARS)[3], first observed in 1965 and formalized in the 1970s, exemplifies this approach. It involves the interaction of pump, Stokes, and probe beams to generate a blue-shifted anti-Stokes signal[5-6], providing chemical specificity without labeling. This paper evaluates the underpinning theory, drawing from historical reviews and modern extensions, to assess its validity, assumptions, and practical implications. We examine core principles, experimental validations, limitations, and recent innovations, emphasizing how the theory enables applications while acknowledging ongoing challenges like NRB interference.

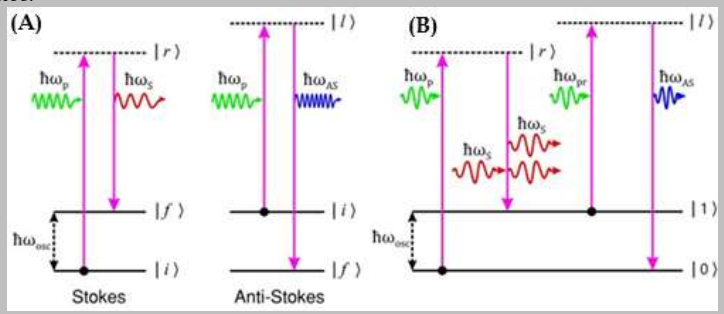

Figure (1): (A) Spontaneous Raman Scattering. (B) Coherant Anti-Stokes Raman Scattering

How to cite this article:

Ahmed, A. N. (2025). Evaluating the Theory Underpinning Nonlinear Raman Spectroscopy Methods: Stimulated Raman Scattering (SRS)and Coherent Anti-Stokes Raman Scattering (CARS). International Journal of Engineering Research for Sustainable Development, 1(6), 67–71. https://doi.org/10.5281/zenodo.18277118

Mathematical Foundations of SRS in Nonlinear Raman Spectroscopy:

The theoretical framework of SRS is built on nonlinear optics, specifically the third-order susceptibility $\chi^{(3)}$, which describes the polarization induced by intense fields[17-19]. Classically, the induced polarization P includes nonlinear terms:

$P = \varepsilon_0 [\chi^{(1)} E + \chi^{(2)} E^2 + \chi^{(3)} E^3 + ...]$

For SRS, the relevant term is $P^{(3)} = \varepsilon_0 \chi^{(3)} E_p^2 E_S^*$, where E_p and E_S are the pump and Stokes fields.

Cross-Section Derivations:

A key aspect is the estimation of spontaneous and stimulated Raman cross-sections[23]. The spontaneous Raman cross-section σ_R is derived as:

$$\sigma_R = \frac{8\pi}{3} \frac{(1 + 2\rho)}{(1 + \rho)} \left(\frac{d\sigma_R}{d\Omega}\right)_{||+perpendicular}$$

where ρ is the depolarization ratio. For SRS, the cross-section σ_{SRS} relates to σ_R via:

$$\sigma_{SRS} = \frac{3\pi\sigma_R c^2 \omega_p}{(1 + 2\rho)\Gamma \omega_s^3}$$

With Γ as the linewidth. This derivation assumes a homogeneous sample and shows reasonable agreement with single-molecule treatments, differing by factors of 2–4 due to focal area approximations.

Three-Wave Resonant Interaction Model:

SRS is modeled as a degenerate 3-wave resonant interaction (3WRI), with equations:

$$\frac{\partial A_1}{\partial x} = -\chi A_2$$
$$\frac{\partial A_2}{\partial x} = -\chi^* A_1$$
$$\frac{\partial \chi}{\partial r} + \gamma \chi = A_1 A_2^*$$

Where A_1 and A_2 are pump and Stokes envelopes, χ is the material excitation, and γ is damping. Neglecting damping yields soliton solutions, such as

$$A_1 = \frac{A(\tau)\, e^{i\varphi}}{coshZ} \; and \; A_2 = A(\tau) tanhZ$$

Highlighting transient effects where solitons deposit energy in the medium.

Raman Gain and Signal Equations:

The Raman gain g_R is:

$$g_R = \frac{8\pi^3 \omega_S}{c^2 n^2} I_m[\chi_{RS}^{(3)}] |E_p|^2$$

Signal changes are approximated as $\Delta I_S \approx g_R I_{p,0} I_{S,0} \Delta z$ for low-loss conditions. where $I_{p,0}$and $I_{S,0}$ are the initial pump and Stokes beams intensities, respectively. As for the Raman interaction length, in many cases, this length can be evaluated similarly to the evaluation of the Rayleigh length.

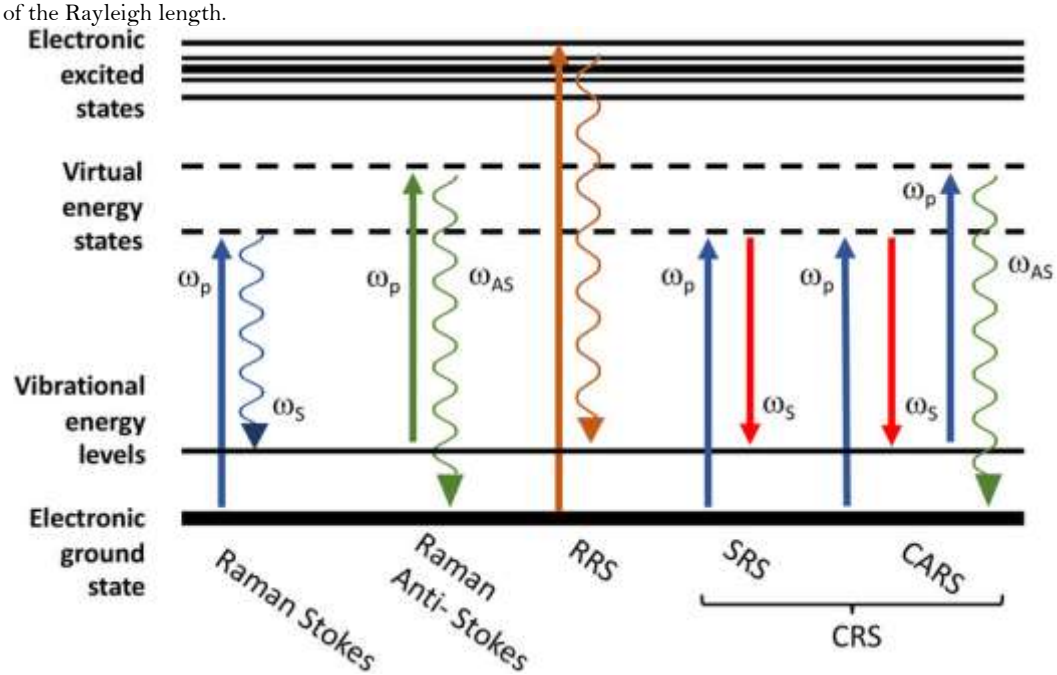

Figure (2): Schematic representation of the energy level diagram of Raman.

Evaluation of the Theory:

The theory of SRS is evaluated through its predictive power, comparisons with experiments, and contrasts with other Raman techniques.

- Sensitivity and Speed: SRS achieves quantum-limited detection with cross-sections up to 10^{-26} cm², enabling single-molecule imaging and video-rate speeds (30 fps) [3-4,15].
- Label-Free Capability: Provides chemical specificity without fluorophores, ideal for biological samples.
- Broadband Coverage: Covers 0 to 4000 cm^{-1} with minimal background.

- Validation: Cross-section derivations align with experimental data, confirming numerical aperture (NA) independence in microscopy.

Restrictions:

- Photodamage: Intensities is greater than 10^{10} W/cm² can heat samples, limiting live-cell use.
- Non-Resonant Background: Reduces SNR by 10 to 100 in some media.
- Phase-Matching: Strict requirements limit turbid media applications.
- Transient Effects: Solitons vanish in finite pulses, complicating long-pulse predictions.
- CARS offers 10^5–10^{10} times stronger signals than spontaneous Raman, enabling fast, label-free imaging with inherent 3D sectioning.
- It separates from fluorescence and works in fluorescing or dilute samples. However, NRB distorts line shapes, reducing sensitivity for weak modes, and requires complex retrieval methods. F_s pulses increase NRB, while p_s pulses limit resolution; high powers risk damage.
- The theory's validity is supported by matching experimental spectra in gases and solids, with $\chi^{(3)}$ models accurately predicting intensities in phase-matched conditions. However, NRB assumptions (real, constant) falter in varying media, leading to distortions; KK/MEM retrievals recover Raman signals but suffer edge errors in discrete implementations. Gaussian pulse models evaluate time-resolved suppression, showing enhancements at delays > t_{FWM}, validated against pyridine data. Surrogate approximations extend theory for fast fitting, reducing errors in combustion (median < 2 K temperature). Learned-matrix approaches improve retrieval accuracy by 3–8 orders in MSE, addressing discretization flaws. Overall, the theory is robust for resonant enhancements but requires refinements for broadband/NRB challenges.

Comparisons with Other Techniques:

The following table compares SRS with spontaneous Raman and CARS:

Aspect	Spontaneous Raman	SRS	CARS
Coherence	Incoherent	Coherent	Coherent
Signal Strength	Weak (10^{-6} of incident)	Amplified (exponential gain)	Strong (10^{-5}–10^{6} enhancement)
Background	Fluorescence possible	Minimal non-resonant	Significant non-resonant
Speed	Slow (long integration)	Fast (video-rate)	Fast, but background distorts
Applications	Bulk analysis	Label-free microscopy	High-speed imaging with phase-matching
Limitations	Low sensitivity	High intensity needed	Spectral distortion

SRS is generally more sensitive than spontaneous Raman (efficiency 10^{-6} vs. 10^{-1}) but lacks CARS's blue-shifted signal advantage.

Counterarguments include CARS's higher signal in some setups, but SRS's background-free nature makes it preferable for quantitative work.

Theoretical Foundations of CARS:

The theory of is rooted in nonlinear optics, specifically third-order processes described by the susceptibility tensor $\chi^{(3)}$. In the semiclassical framework, the induced polarization $P^{(3)}$ drives the anti-Stokes field, with the intensity

$I_{CARS} \propto |\chi^{(3)}|^2 I_p^2 I_S$,

where I_p and I_S are pump and Stokes intensities. $\chi^{(3)}$ decomposes into resonant ($\chi^{(3)}_R$, complex Lorentzian) and non-resonant ($\chi^{(3)}_{NR}$, real) components, leading to interference that distorts spectra. The resonant part is

$$\chi_R^{(3)} = \sum \frac{A_k}{\Omega - \Omega_k + i\,\Gamma_k}$$

Where Ω is the Raman shift, Ω_k the mode frequency, and Γ_k the linewidth. Phase-matching ($\Delta k \approx 0$) is critical, with geometries like collinear (gases) or folded boxcars (liquids) ensuring coherence. In the transient grating (T_G) picture, pump and Stokes create a moving refractive index modulation, probed to yield the signal. For ultrashort Gaussian pulses, closed-form solutions using the Faddeeva function describe time-resolved signals, enabling NRB suppression via probe delays. Quantum treatments incorporate exciton resonances, as in carbon nanotubes, extending the theory to electronic-vibrational coupling[11].

Experimental Configurations:

CARS setups typically use Ti : sapphire lasers or fiber-based sources for pump (narrowband, p_s) and Stokes (broadband, f_s) beams, synchronized via delay lines[16]. Multiplex/broadband variants employ supercontinuum Stokes for wide spectral coverage (up to 4000 cm^{-1}), with detection in forward (F-CARS) or epi (E-CARS) modes. In microscopy, high-NA objectives focus beams for 3D imaging, with video-rate capabilities using p_s pulses. Dual-pump configurations enable multi-species detection in combustion.

Technique	Signal Strength	Spectral Resolution	NRB Interference	Speed	Applications
Spontaneous Raman	Low (10^{-29} cm^2/molecule)	High (~1cm^{-1})	None	Slow (long integration)	General spectroscopy
CARS	High (coherent, 10^5–10^{10})	Medium (~1–10cm^{-1})	High (distorts spectra)	Fast (video-rate)	Imaging, combustion
SRS	High (coherent)	High (~1 cm^{-1})	Low (background-free)	Fast	Biomedical imaging
BCARS	High, broadband	Medium-wide (200–4000cm^{-1})	High, but retrievable	Medium-fast	Hyperspectral materials

Applications:

- Microscopy: Real-time lipid and protein imaging in cells.
- Materials Science: Defect analysis in semiconductors.

- Biomedicine: Cancer diagnostics via tissue mapping. Integrations like epi-SRS enhance deep-tissue penetration[24].
- In biomedicine, CARS images lipids in cells/tissues, tracking droplets in adipocytes or myelin in nerves. In materials, it maps polymers and catalysts.
- Combustion diagnostics use dual-pump CARS for temperature/species mapping in flames[22].
- Broadband variants enable hyperspectral analysis of crystals like SiC or domain walls in ferroelectrics[7].

Conclusion:

The theory of SRS in nonlinear Raman spectroscopy is well-substantiated, offering superior sensitivity and versatility. However, limitations like photodamage warrant ongoing refinements, such as quantum light integration. Future work may address controversies in cross-section discrepancies for broader adoption.

Recent Advances: Chirped-pulse CARS maximizes vibrational coherence. BCARS with KK retrieval achieves reproducibility across setups, validating theory in materials[14]. Quantum control and exciton-resonant CARS extend to nanostructures. Kernel-based surrogates accelerate diagnostics[20-21].

The theory underpinning CARS effectively explains nonlinear Raman processes, enabling diverse applications, though NRB and discretization issues warrant ongoing evaluation. Future refinements in pulse shaping and AI-driven retrievals promise enhanced accuracy.

Acknowledgment

I am Dr. Abullais Nehal Ahmed, thankful to the Principal, J.A.T., Arts, Sci., and Comm. College (for Women), Malegaon, Dist.Nashik. for granting permission to carry out this project.

Financial support and sponsorship

Nil.

Conflicts of interest

The authors declare that there are no conflicts of interest regarding the publication of this paper

References:

1. Ozeki Y, Dake F, Kajiyama S, Fukui K, Itoh K. Analysis and experimental assessment of the sensitivity of stimulated Raman scattering microscopy. *Optic Express* (2009) 17(5):3651–8. doi:10.1364/OE.17.003651
2. Chen BC, Sung J, Wu X, Lim SH. Chemical imaging and micro-spectroscopy with spectral focusing coherent anti-Stokes Raman scattering. *J Biomed Optic* (2011) 16(2):021112. doi:10.1117/1.3533315
3. Hashimoto K, Omachi J, Ideguchi T. Ultra-broadband rapid-scan Fourier-transform CARS spectroscopy with sub-10-fs optical pulses. *Optic Express* (2018) 26(11):14307–14. doi:10.1364/OE.26.014307
4. Parekh SH, Lee YJ, Aamer KA, Cicerone MT. Label-free cellular imaging by broadband coherent anti-Stokes Raman scattering microscopy. *Biophys J* (2010) 99(8):2695–704. doi:10.1016/j.bpj.2010.08.009
5. Gu M, Satija A, Lucht RP. Impact of moderate pump–Stokes chirp on femtosecond coherent anti-Stokes Raman scattering spectra. *J Raman Spectrosc* (2020) 51(1):115–24. doi:10.1002/jrs.5754
6. 3 Fu D, Holtom G, Freudiger C, Zhang X, Xie XS. Hyperspectral imaging with stimulated Raman scattering by chirped femtosecond lasers. *J Phys Chem B* (2013) 117(16):4634–40. doi:10.1021/jp308938t
7. 20 Liu Y, Lee YJ, Cicerone MT. Broadband CARS spectral phase retrieval using a time-domain Kramers-Kronig transform. *Opt Lett* (2009) 34(9):1363–5. doi:10.1364/OL.34.001363
8. Zhang C, Cheng J-X. Perspective: coherent Raman scattering microscopy, the future is bright. *APL Photonics* (2018) 3(9):090901. doi:10.1063/1.5040101.
9. Rigneault H, Berto P. Tutorial: coherent Raman light matter interaction processes. *APL Photonics* (2018) 3(9):091101. doi:10.1063/1.5030335.
10. Segawa H, Okuno M, Kano H, Leproux P, Couderc V, Hamaguchi HO. Label-free tetra-modal molecular imaging of living cells with CARS, SHG, THG and TSFG (coherent anti-Stokes Raman scattering, second harmonic generation, third harmonic generation and third-order sum frequency generation). *Optic Express* (2012) 20(9):9551–7. doi:10.1364/OE.20.009551.
11. Kiss N, Krolopp Á, Lőrincz K, Bánvölgyi A, Szipőcs R, Wikonkál N. Stain-free histopathology of basal cell carcinoma by dual vibration resonance frequency cars microscopy. *Pathol Oncol Res* (2018) 24(4):927–30. doi:10.1007/s12253-017-0356-6.
12. Chen W-W, Lemieux GA, Camp CH, Chang T-C, Ashrafi K, Cicerone MT. Spectroscopic coherent Raman imaging of *Caenorhabditis elegans* reveals lipid particle diversity. *Nat Chem Biol* (2020) 16:1087–95. doi:10.1038/s41589-020-0565-2.
13. Hiramatsu K, Ideguchi T, Yonamine Y, Lee S, Luo Y, Hashimoto K, et al. High-throughput label-free molecular fingerprinting flow cytometry. *Sci Adv* (2019) 5(1):eaau0241. doi:10.1126/sciadv.aau0241.
14. Gong L, Zheng W, Ma Y, Huang Z. Higher-order coherent anti-Stokes Raman scattering microscopy realizes label-free super-resolution vibrational imaging. *Nat Photon* (2019) 14:115–22. doi:10.1038/s41566-019-0535-y.
15. Heuke S, Sivankutty S, Scotte C, Stockton P, Bartels RA, Sentenac A, et al. Spatial frequency modulated imaging in coherent anti-Stokes Raman microscopy. *Optica* (2020) 7(5):417–24. doi:10.1364/Optica.386526.
16. Kong C, Pilger C, Hachmeister H, Wei X, Cheung TH, Lai CSW, et al. High-contrast, fast chemical imaging by coherent Raman scattering using a self-synchronized two-colour fibre laser. *Light Sci Appl* (2020) 9(1):25. doi:10.1038/s41377-020-0259-2.
17. Tai B. *Fiber-based high energy ultrafast sources for nonlinear microscopy*. [PhD thesis]. Ann Arbor (MI): Boston University (2019).
18. Yarbakht M, Pradhan P, Köse-Vogel N, Bae H, Stengel S, Meyer T, et al. Nonlinear multimodal imaging characteristics of early septic liver injury in a mouse model of peritonitis. *Anal Chem* (2019) 91(17):11116–21. doi:10.1021/acs.analchem.9b01746.
19. Meyer T, Bae H, Hasse S, Winter J, Woedtke TV, Schmitt M, et al. Multimodal nonlinear microscopy for therapy monitoring of cold atmospheric plasma treatment. *Micromachines* (2019) 10(9). doi:10.3390/mi10090564.
20. Li R, Wang X, Zhou Y, Zong H, Chen M, Sun M. Advances in nonlinear optical microscopy for biophotonics. *J Nanophotonics* (2018) 12(3):033007. doi:10.1117/1.JNP.12.033007.

21. Bozsányi S, Farkas K, Bánvölgyi A, Lőrincz K, Fésűs L, Anker P, Zakariás S, Jobbágy A, Lihacova I, Lihachev A, Lange M, Bliznuks D, Medvecz M, Kiss N, Wikonkál NM.Diagnostics (Basel). 2021 Jul 22;11(8):1315. doi: 10.3390/diagnostics11081315.
22. Delrue C, Speeckaert R, Oyaert M, De Bruyne S, Speeckaert MM.J Clin Med. 2023 Nov 30;12(23):7428. doi: 10.3390/jcm12237428.
23. Anker P, Fésűs L, Kiss N, Lengyel A, Pinti É, Lihacova I, Lihachev A, Plorina EV, Fekete G, Medvecz M.Diagnostics (Basel). 2023 Jul 14;13(14):2368. doi: 10.3390/diagnostics13142368.
24. Mazumder N, Balla NK, Zhuo GY, Kistenev YV, Kumar R, Kao FJ, et al. Label-free non-linear multimodal optical microscopy-basics, development, and applications. *Front Phys* (2019) 7:170. doi:10.3389/fphy.2019.00170.